Preprints.org

Article

Not peer-reviewed version

Enhanced Antibacterial Activity of Vancomycin Loaded on Functionalized Polyketones

Rachele Rampazzo , Andrea Vavasori * , Lucio Ronchin , Pietro Riello , Martina Marchiori , Gloria Saorin , Valentina Beghetto *

Posted Date: 19 June 2024

doi: 10.20944/preprints202406.1370.v1

Keywords: Polyketone, Paal-Knorr, Vancomycin, Antibiotics, Drug delivery

Preprints.org is a free multidiscipline platform providing preprint service that is dedicated to making early versions of research outputs permanently available and citable. Preprints posted at Preprints.org appear in Web of Science, Crossref, Google Scholar, Scilit, Europe PMC.

Copyright: This is an open access article distributed under the Creative Commons Attribution License which permits unrestricted use, distribution, and reproduction in any medium, provided the original work is properly cited.

Preprints.org (www.preprints.org) | NOT PEER-REVIEWED | Posted: 19 June 2024 doi:10.20944/preprints202406.1370.v1

Disclaimer/Publisher's Note: The statements, opinions, and data contained in all publications are solely those of the individual author(s) and contributor(s) and not of MDPI and/or the editor(s). MDPI and/or the editor(s) disclaim responsibility for any injury to people or property resulting from any ideas, methods, instructions, or products referred to in the content.

Article

Enhanced Antibacterial Activity of Vancomycin Loaded on Functionalized Polyketones

Rachele Rampazzo [1,2], Andrea Vavasori [1]*, Lucio Ronchin [1], Pietro Riello [1], Martina Marchiori [1], Gloria Saorin [1] and Valentina Beghetto [1,3,4]*

[1] Department of Molecular Sciences and Nanosystems, University Ca' Foscari, Venice, Via Torino5 155, 30172 Mestre, Italy.
[2] Rachele Rampazzo, Department of Architecture and Industrial Design, University of Campania "Luigi Vanvitelli", Aversa, Italy
[3] Crossing S.r.l., Viale della Repubblica 193/b, 31100 Treviso, Italy; valentina.beghetto@crossing-srl.com
[4] Consorzio Interuniversitario per le Reattività Chimiche e la Catalisi (CIRCC), via C. Ulpiani 27, 701268 Bari, Italy
* Correspondence: andrea.vavasori@unive.it; (A.V.); valentina.beghetto@unive.it (V.B.); Tel.+390412348928.

Abstract: Today, polymeric Drug Delivery Systems (DDS) appear as an interesting solution against bacterial resistance, having great advantages such as low toxicity, biocompatibility, and biodegradability. In this work, two polyketones (PK) have been post-functionalized with taurinate (PKT) or sulfanilate (PKSK) and employed as biocompatible carriers for Vancomycin against bacterial infections. Modified PKs were easily prepared by Paal-Knorr reaction and loaded with Vancomycin at variable pH. All polymers were characterized by FT-IR, DSC, TGA, SEM and elemental analysis. Antimicrobial activity was tested against Gram positive Staphylococcus aureus ATCC 25923 and correlated to the different pH used for its loading (between 2.3 and 8.8). Distinctively, minimum inhibitory concentrations achieved with PKT and PKSK loaded with Vancomycin are similar, 0.23μg/mL and 0.24μg/mL respectively, i.e. six times lower that Vancomycin alone. The use of post-functionalized aliphatic polyketones has thus been demonstrated to be a promising way to obtain very efficient polymeric DDS.

Keywords: Polyketone; Paal-Knorr; Vancomycin; Antibiotics; Drug delivery

1. Introduction

Today, the fight against infectious diseases still poses a serious challenge worldwide for healthcare. According to the literature, bacteria are becoming quickly resistant to commercially available antibiotics and antiseptics [1-7]. Antibiotics are often used in massive doses to maintain their therapeutic effects because of their low bioavailability and unfavorable interactions with biological barriers promoting bacterial resistance. Moreover, resistant bacteria develop different mechanisms such as efflux pumps [8-10], inactivation of enzymes expression [10-12], modification of drug penetration through barriers [10,13], further reducing antibiotic efficiency. Additionally, bacteria may promote biofilm formation, which is a protective self-produced extracellular polymeric matrix, contributing to their difficult eradication [14-16]. Therefore, a deep comprehension of resistance mechanisms and the development of alternative antimicrobials are necessary to address the problem of bacteria resistance [1,17-22].

Drug Delivery Systems (DDS) are widely used to prevent antibiotics and antiseptics resistance, improving drugs efficiency, selectivity, biodistribution and pharmacokinetics, and preventing biofilm formation [6,23-32]. Biocompatible materials, such as polymers, polysaccharides, proteins, lipids, and peptides are widely used to produce DDS, avoiding drug degradation and adverse effects, controlling drug release [6,33-38].

© 2024 by the author(s). Distributed under a Creative Commons CC BY license.

Preprints.org (www.preprints.org) | NOT PEER-REVIEWED | Posted: 19 June 2024 doi:10.20944/preprints202406.1370.v1

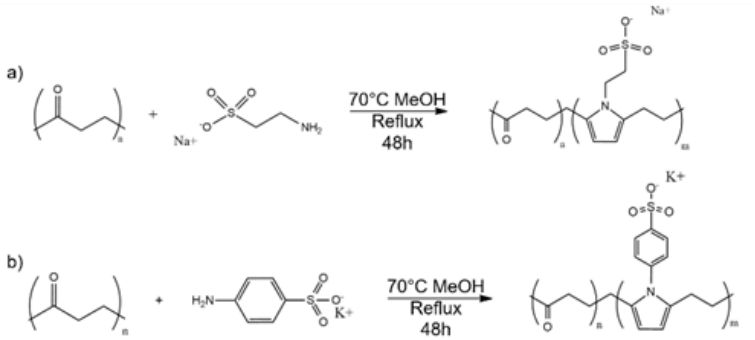

Scheme 1. Synthetic scheme for the preparation of post-functionalized PK with a) taurinate (PKT) and b) sulfanilate (PKSK).

Specifically devised polymers are also a promising alternative for biomedical and biotechnological applications, synthesized with different functional groups, promoting interactions with drugs [34,35,39-46]. DDS based materials can be used as carriers of therapeutic molecules (nanoparticles, microparticles, implants) or as conjugates, bonding drug molecules through linkers designed to release them specifically on targeted sites [10,34,39,47-51]. To date, DDS prepared with biocompatible polymers have been widely described in the literature and many are also commercially available [52-54].

Within this panorama, aliphatic PK appear as an interesting yet scantly explored solution as polymeric carriers for DDS production [55,56]. In fact, aliphatic PK, produced by catalytic copolymerization of CO and ethylene, may be easily post-functionalized by means of the so-called Paal-Knorr reaction [57], allowing to obtain customized PK with specific desired functional groups [58-71].

Even though few works have been published in the literature on the preparation of post-functionalized PK, data reported in the literature demonstrate their high potential as supports for different types of enzymes [72], germicide polymeric coatings[73] or as scaffolds for urothelial cells [56].

Vancomycin (VCM), a branched tricyclic glycosylated peptide antibiotic (Figure 1), is a very interesting last line defense antibiotic used against serious infections caused by Staphylococci, Enterococci, and other Gram-positive pathogenic bacteria [74-83], inhibiting cell wall synthesis in sensitive bacteria. Because of its wide use, to limit the rise of bacterial resistance to VCM, development of DDS is fundamental.

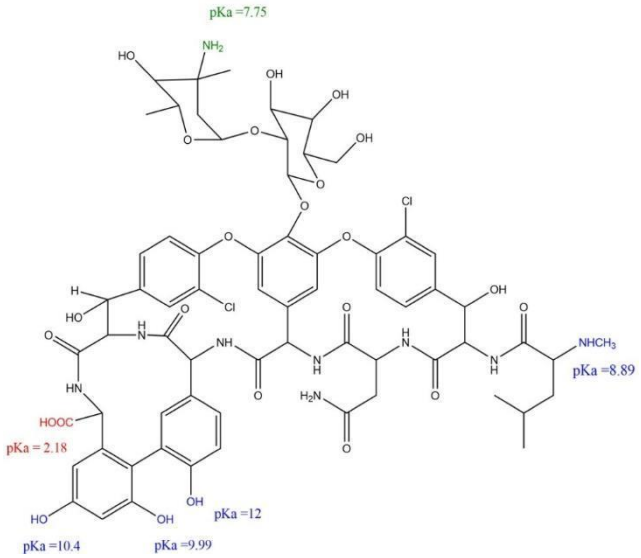

Figure 1. Molecular structure of Vancomycin.

Physical chemical studies have demonstrated that VCM polymeric formulations are able to penetrate the bacterial phospholipidic double membrane by releasing the drug locally, inhibiting

Preprints.org (www.preprints.org) | NOT PEER-REVIEWED | Posted: 19 June 2024 doi:10.20944/preprints202406.1370.v1

biofilm formation and eradicating mature biofilms [14,38,84-89]. In this context, the aim of this work is to prepare polymeric DDS employing specifically customized PK able to interact with VCM through ionic and hydrophobic bonds [38,90,91]. PK was prepared according to literature procedure [68], post functionalized with sulfanilate (PKSK) or taurinate (PKT) and loaded with Vancomycin (VCM) at different pH. All polymers were characterized by FT-IR, DSC, TGA, SEM, elemental analysis, while NMR analysis was not performed due to the insolubility of PKs, even after functionalization. PKSK and PKT before and after VCM loading were further tested against *Staphylococcus aureus* ATCC 25923 strain and their antimicrobial activity compared to pure VCM.

2. Materials and Methods

Carbon monoxide and ethene were supplied by SIAD Company Italy ("research grade", purity > 99.9%). Bis(diphenylphosphino)propane (Dppp), TsOH (p-toluene sulfonic acid), Methanol (99.8%), Diethyl ether (>99.5 %), Sulfanilic acid (≥ 98%), Taurine (≥99 %), Sodium hydroxide (≥98 %), Potassium hydroxide (≥85 %), m-Cresol (99 %), Dimethyl sulfoxide (99%), Agar, Phosphate-buffered saline (PBS), Nutrient broth (NB), Mueller Hinton Broth (MHB) and Vancomycin hydrochloride were purchased from Sigma Aldrich Co. (St. Louis, MO). MilliQ water was used for all experiments. The complexes $[Pd(OAc)_2(dppp)]$ were prepared as reported in literature [92]. Staphylococcus aureus ATCC 25923 strain was obtained from the American Type Culture Collection. 96-Well Microtiter Microplates was purchased from Thermo Fisher.

The average viscosity molecular weight of PK has been evaluated as Limit Viscosity Number (LVN), used m-cresol as solvent and the viscosity was measured by a Cannon-Fenske type capillary viscosimeter, thermostated at 25°C, as reported in literature [93].

FT-IR spectroscopy was measures on a Nicolet AVATAR Nexus FT-IR Thermo Fisher Scientific spectrometer in KBr, with 32 scans and a resolution of 4 cm^{-1} in the wave number range between 4000 cm^{-1} and 400 cm^{-1}. The melting and decomposition temperature and thermogravimetric analysis of polymers was determined using a DSC/TGA Linseis PTA ST1000 under nitrogen flow of 100 mL/ min with a temperature ramp of 20 °C min^{-1} from 30 °C to 500 °C. Elemental analysis for carbon, hydrogen, nitrogen, oxygen, and sulphur (CHNSO) were performed using UNICUBE organic elemental analyzer (Elemental). It offers highly sensitive analysis at a detection limit of 10 µg/g or 10 ppm. UV-Vis spectra were recorded on UV Carey 100 (Agilent) spectrophotometer in a grass cuvette in the range 400 – 200 cm^{-1}. Scanning electron microscopy (SEM) was carried out with a Zeiss Sigma|VP (Jena, Germany), variable pressure instrument (VP-SEM), at 20 kV and variable magnifications. For SEM imaging, the samples were prepared by Au deposition (layer about 40 nm) using AC sputtering.

Optical density measurement (OD600) was conducted by BioTek Synergy H1 a modular multimode microplate reader, with monochromator-based optics and filter-based optics. The optical density at 600 nm is referred to as OD600. The light at λ=600 nm is easy to produce and does little to damage or hinder microbial growth.

2.2. Synthesis of Aliphatic Polyketones (PK)

The reaction was conducted in a 250 mL stainless steel autoclave equipped using a 150 mL Pyrex glass beaker. In typical experiment, 2.10 mg of $[Pd(OAc)_2(dppp)]$ (0.003 mmol), 246.23 mg of *p*-TsOH (1.29 mmol) and 60 mL of methanol were mixed in a 150 mL Pyrex glass beaker, and then placed in the autoclave. The autoclave was then sealed and pressurized with a 1/1 mixture of CO/C_2H_4 at 5.0 MPa and heated to 90 °C for 4 hours over stirring. After cooling to room temperature, a solid product was collected, filtered, and washed three times with methanol, acetone and diethyl ether. The resulting white powder polyketone (PK) was dried in vacuum for approximately 8 hours [92-96]. M.p. 250 °C; FT-IR (KBr, cm^{-1}): ν˜= 1690 (vs) (C=O), 2900 (s) (C-H), 1406 (s) (C-H), 1333 (s) (C-H), 1057 (s) (C-H); Elemental analysis (%) for PK found: C 63.45, H 7.06, 0 29.49.

2.3. Synthesis of PKSK and PKT by Paal-Knorr Modification of PK with Potassium Sulfanilate Or Sodium Taurinate

Preprints.org (www.preprints.org) | NOT PEER-REVIEWED | Posted: 19 June 2024 doi:10.20944/preprints202406.1370.v1

In a round-bottom flask equipped with a mechanical stirrer and a reflux condenser, 1.0 g of polyketone (PK) was suspended in 30 mL of methanol with 1.88g potassium sulfanilate (0.09 mol) or 1.3g sodium taurinate (0.09 mol). The reaction mixture was heated at 70 °C for 48h, and after cooling was collected by filtration, washed with methanol, acetone and diethyl ether. The resulting brown powder polyketone with potassium sulfanilate (PKSK) and orange powder polyketone with sodium taurinate (PKT) were dried in a vacuum for 8 hours and characterized by FT-IR, DSC, TGA, Elemental analysis, SEM and OD600[96-100].

PKSK: M.p. 234ºC; FT-IR (KBr, cm^{-1}): ν̃= 685 (s), 813 (w), 832 (w), 1010 (s), 1035 (s), 1057 (w), 1124 (s), 1164 (s), 1246 (s), 1259 (w), 1335 (w), 1408 (s), 1426 (w), 1499 (s), 1693 (vs), 2852 (w, br), 2912 (w, br), 2963 (w), 3437 (vs, br), (see Table 1S in supporting information); Elemental analysis (%) for PKSK found: C 51.18, H 5.38, N 4.02, S 9.31.

PKT: M.p. 214ºC; FT-IR (KBr, cm^{-1}): ν̃=812 (w),1054 (s), 1198 (m, br), 1259 (w), 1336 (s), 1409 (s), 1427 (w), 1470 (w), 1693 (vs), 2853 (w), 2913 (w), 2953 (w), 3439 (vs, br), (see Table 2S in supporting information); Elemental analysis (%) for PKT found: C 54.76, H 6.5, N 1.66, S 4.23.

2.4. Loading of Vancomycin on PKSK or PKT

Loading of VCM on functionalized polyketones (PKSK or PKT) following the same protocol and the sensitiveness to pH was evaluated in DMSO solutions, in the 2.3-5.0-8.8 pH range (obtained by HCl or NaOH solutions respectively) (pH 8+ DSA potentiometer, favs Scientific Equipment) at room temperature. Polymer and Vancomycin 2/1 wt/wt ratio were suspended in 2mL DMSO (pH 2.3,5.0,8.8) under stirring. After 20 min, the solution was dialysed against MilliQ water with Spectra/Por 1 Dialysis Membrane Standard RC Tubing MWCO: 6 – 8 kD for 24 h to remove the remained unabsorbed antibiotic. The concentration of unabsorbed antibiotic (Free-VCM) resulted in the MilliQ water was measured using UV at a wavelength of 281 nm [101-103]. VCM encapsulation efficiency % (EE%) and loading capacity % (LC%) were determined as follow:

$$EE\% = \frac{TotalVCM - FreeVCM}{TotalVCM} x100$$

$$LC\% = \frac{TotalVCM - FreeVCM}{Polymer + (TotalVCM - FreeVCM)} x100$$

Total VCM = the starting VCM amount used for the loading.

Polymer = the starting PKSK or PKT amount used for the loading considering no losses.

Samples were lyophilized and characterized by FT-IR, DSC, TGA, SEM, OD600.

PKSK-VCM pH 2.3: M.p. 234 °C; FT-IR (KBr, cm^{-1}): ν̃= 806 (w), 1015 (w), 1035 (w), 1057 (m), 1124 (w), 1195 (w, br), 1260 (w), 1335 (m), 1408 (s), 1426 (w), 1499 (w), 1693 (vs), 2852 (w), 2912 (w), 2963 (w), 3437 (s, br) (see Table 1S in supporting information); Elemental analysis (%) for PKSK-VCM pH 2.3 found: C 50.87, H 4.96, N 4.36, S 7.67.

PKSK-VCM pH 5.0: M.p. 234 °C; FT-IR (KBr, cm^{-1}): ν̃= 806 (w), 1015 (w), 1035 (w), 1057 (m), 1124 (m), 1195 (m, br), 1260 (w), 1335 (m), 1384 (w), 1408 (s), 1426 (w), 1499 (w), 1693 (vs), 2852 (w), 2912 (w), 2963 (w), 3437 (s, br), (see Table 1S in supporting information); Elemental analysis (%) for PKSK-VCM pH 5.0 found: C 47.38, H 3.87, N 7.13, S 2.37.

PKSK-VCM pH 8.8: M.p. 234 °C; FT-IR (KBr, cm^{-1}): ν̃= 806 (m), 1015 (w), 1035 (w), 1057 (m), 1124 (w), 1195 (w, br), 1260 (m), 1335 (m), 1384 (s), 1408 (s), 1426 (w), 1499 (w), 1693 (vs), 2852 (w), 2912 (w), 2963 (w), 3437 (vs, br), (see Table 1S in supporting information); Elemental analysis (%) for PKSK-VCM pH 8.8 found: C 48.76, H 4.28, N 5.86, S 5.10.

PKT-VCM pH 2.3: M.p. 214 °C; FT-IR (KBr, cm^{-1}): ν̃=812 (m), 1023 (w), 1054 (s), 1095 (w, br), 1198 (w, br), 1259 (w), 1336 (m), 1384 (w), 1409 (s), 1427 (w), 1470 (w), 1693 (vs), 2852 (w), 2918 (w), 2962 (w), 3439 (vs, br) (see Table 2S in supporting information); Elemental analysis (%) for PKT-VCM pH 2.3 found: C 53.14, H 5.63, N 2.10, S 3.75.

PKT-VCM pH 5.0: M.p. 214 °C; FT-IR (KBr, cm^{-1}): ν̃=812 (m), 1023 (w), 1054 (s), 1095 (w, br), 1198 (w, br), 1259 (w), 1336 (m), 1384 (w), 1409 (s), 1427 (w), 1470 (w), 1693 (vs), 2852 (w), 2918 (w),

Preprints.org (www.preprints.org) | NOT PEER-REVIEWED | Posted: 19 June 2024 doi:10.20944/preprints202406.1370.v1

2962 (w), 3439 (vs, br), (see Table 2S in supporting information); Elemental analysis (%) for PKT-VCM pH 5.0 found: C 49.35, H 3.46, N 7.73, S 1.12.

PKT-VCM pH 8.8: M.p. 214 °C; FT-IR (KBr, cm^{-1}): ν˜=812 (m), 1023 (w), 1054 (s), 1095 (w, br), 1198 (w, br), 1259 (w), 1336 (m), 1384 (w), 1409 (s), 1427 (w), 1470 (w), 1693 (vs), 2852 (w), 2918 (w), 2962 (w), 3439 (vs, br), (see Table 2S in supporting information); Elemental analysis (%) for PKT-VCM pH 8.8 found: C 52.78, H 4.71, N 3.66, S 3.41.

2.5. Vancomycin Release

Vancomycin release from PKT-VCM and PKSK-VCM was assessed using test tubes containing 5.0 mL of PBS phosphate buffer pH 7.4 with 5.0 mg of samples and thermostated at 37 °C. The experiments were carried out in triplicate (without stirring) under sink conditions. Released antibiotics were quantified by UV at a wavelength of 281 nm [99,103,104].

2.6. Antibacterial Activity

Antimicrobial activity was determined by standard liquid dilution method in Nutrient broth (NB) medium. S. aureus ATCC 25923 cells were grown overnight at 37 °C in NB broth and diluted in the same medium for assays. In 96-well sterile microtiter tray, 50 µL of bacteria from overnight culture (adjusted to 1x106 cells/mL) was added to the serial dilution of PKT-VCM and PKSK-VCM from 25 µg/ml and final concentration of 0 mg/ml as blank, in a total volume of 150 µl of NB. The 96-well microtiter tray was incubated at 37°C, overnight, in a shaking incubator and the cells growth was assessed by measuring OD at 600 nm. MICs (minimum inhibition concentrations) were determined as the lowest antibiotic.

3. Results and Discussion

3.1. Synthesis of Post Functionalized PKs

PK prepared according to literature method [68] (Mw = 15.272 g mol^{-1} determined as reported by Vavasori and coworkers [93]), was post-functionalized by Paal-Knorr reaction in the presence of taurinate or sulfanilate (1/1 molar ratio) at 70 °C, for 48 h in methanol as solvent (Scheme 1a, 1b). After work up (see experimental section), the solid polymers, recovered in high yields (2.3g, 80% and 1.96g, 85% respectively for PKSK and PKT), were characterized by FT-IR, DSC, TGA, SEM and elemental analysis. Taurinate and sulfanilate were chosen to prepare a specific modified PK (PKSK and PKT) containing anionic functional groups, which should promote the interaction and immobilization of VCM

Moreover, it is interesting to note that taurinate and sulfanilate were expected to improve the solubility of the post-functionalized polymers, yet both PKSK and PKT were not soluble in any conventional organic solvent nor in water (at any pH).

3.2. Influence of pH on Vancomycin Loading

To find best loading conditions, it is important to consider that VCM is a large molecule bearing six different acidic and basic functional groups with specific pKa (Figure 1). Thus, VCM is differently charged, going from -4 at pH > 13, to +2 at acidic pH (~0) [105], and consequently its reactivity towards PKSK and PKT will be influenced by the pH.

PKSK and PKT were loaded with VCM at room temperature using a common protocol and operating at three different pH values (2.3, 5.0, 8.8) [104]. Polymers loaded with VCM, named PKSK-VCM and PKT-VCM, were purified by dialysis and unabsorbed VCM measured by UV at 281 nm (Figure 1S) [101-103], to determine encapsulation efficiency (EE%) and loading capacity (LC%) (reported in Table 1; all experiments were performed in triplicate and all data are expressed as the mean ± standard deviation).

Table 1. Elemental analysis of PKT, PKSK, PKT-VCM and PKSK-VCM. EE% and LC% of PKSK-VCM and PKT-VCM.

Preprints.org (www.preprints.org) | NOT PEER-REVIEWED | Posted: 19 June 2024 doi:10.20944/preprints202406.1370.v1

Sample	pH	Elementals(%)		EE%	LC%
		N	S		
PKSK	-	4.02±0.01	9.31±0.02	-	-
PKSK-VCM	2.3	4.36±0.02	7.67±0.01	41.25±0.03	23.08±0.01
PKSK-VCM	5.0	7.13±0.01	2.37±0.03	75.00±0.02	31.03±0.01
PKSK-VCM	8.8	5.86±0.01	5.10±0.01	66.66±0.01	25.00±0.02
PKT	-	1.66±0.03	4.23±0.02	-	-
PKT-VCM	2.3	2.10±0.01	3.75±0.03	23.08±0.01	10.71±0.02
PKT-VCM	5.0	7.73±0.02	1.12±0.01	80.00±0.02	31.58±0.01
PKT-VCM	8.8	3.66±0.03	3.41±0.03	42.67±0.02	15.15±0.03

Data reported in Table 1 show that, with both polymers, maximum LC% and highest EE% were achieved at pH 5.0. These data where further confirmed by elemental analysis, since highest nitrogen content was determined at pH 5.0, confirming the presence of higher amounts of Vancomycin. At pH 2.3 or 8.8, a decrease of EE% of up to 34% for PKSK-VCM and 57% for PKT-VCM and LC% between 8% and 21%, respectively, was registered. According to the literature, at pH 2.3 VCM has the higher positive charge (+2) and therefore this pH was supposed to be the optimal one for the loading on anionic polyketones tested[105]. Nonetheless data reported in Table 1 clearly show that highest VCM loading was obtained at pH 5.0, confirming that not only ionic but also hydrophobic interactions are important to promote VCM loading. Moreover, higher encapsulation efficiency by PKSK-VCM as compared to PKT-VCM, may be attributed to higher hydrophobic interactions between VCM and the aromatic functional groups present in PKSK [38, 90, 91, 106].

3.3. PKT-VCM and PKSK-VCM Characterisation

PKT, PKSK, PKT-VCM and PKSK-VCM were lyophilized and characterized by FT-IR, DSC, TGA, SEM and elemental analysis. FT-IR of PKSK, PKT and PKT-VCM, PKSK-VCM prepared at different pH show very modest differences, and no clear evidence of the presence of VCM in the FT-IR of PKSK-VCM and PKT-VCM could be highlighted, probably due to the very low amount of antibiotic present with respect to the polymer. Nevertheless, comparison of FT-IR of polymers before and after VCM loading show a slight shift of the peaks in the range 1010-1095 cm^{-1}, corresponding to the SO_3^- groups which are the functional groups mostly affected by the loading of VCM (see Figure 2S and Tables 1S, 2S). Additionally, picks corresponding to the aromatic rings present in PKSK also show a modest shift (813-832 cm^{-1} to 806 cm^{-1}), (see Figure 2S and Tables 1S, 2S), suggesting that not only ionic but also hydrophobic interactions may contribute to drug retention [38,90].

To gain further information on the characteristics of polymers prepared, thermal analyses (DSC, TGA) were performed (Figure 3S, Figure 4S). In agreement with the literature [107], due to the very low loading of VCM on the polymers, no significant difference was observed between PKT and PKT-VCM or PKSK and PKSK-VCM.

Preprints.org (www.preprints.org) | NOT PEER-REVIEWED | Posted: 19 June 2024 doi:10.20944/preprints202406.1370.v1

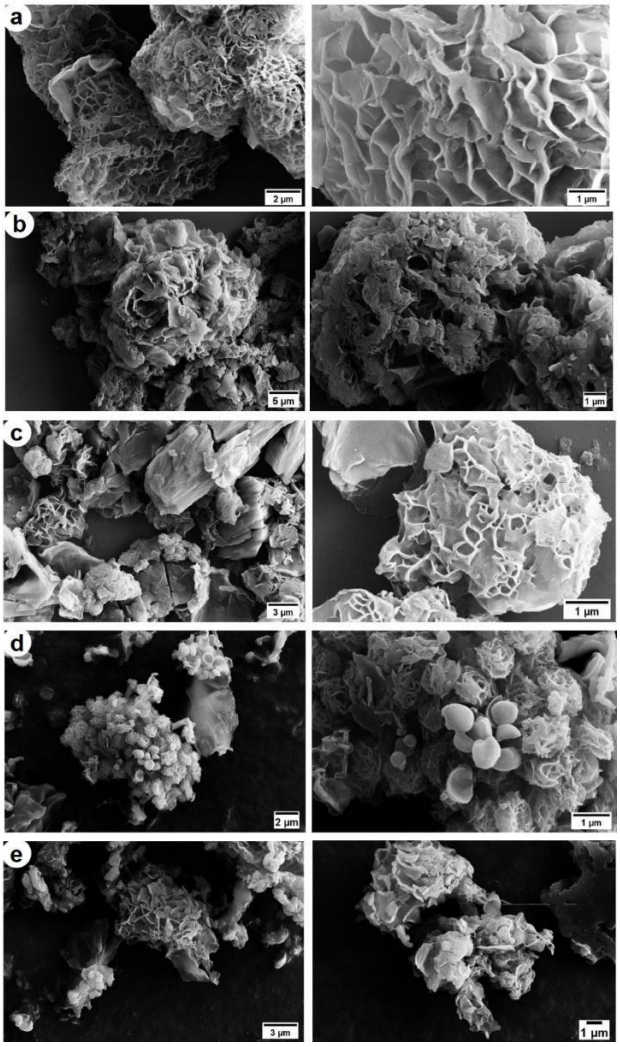

Figure 2. SEM images of a) PK, b) PKT, c) PKSK, d) PKT-VCM (pH 5.0), e) PKSK-VCM (pH 5.0).

Interestingly, SEM analysis of PKT-VCM and PKSK-VCM with higher VCM loading (Table 1), showed evident differences between the polymers before and after VCM loading (Figure 2). The SEM images of PK (Figure 2a) show pores with lamellate edges of average size 1.13 ± 0.05 µm, while on PKT surface (Figure 2b), pores are smoother, less laminated with poorly defined edges (0.48 ± 0.03 µm), probably due to the functionalization of PK with taurinate, leading to morphological changes. Similarly, PKSK images (Figure 2c) showed a different morphology compared to PK, due to the partial functionalization, although also in this case pores were visible (0.25 ± 0.02 µm). When VCM was loaded on PKT or PKSK (Figure 2d and Figure 2e respectively), the morphology of the polymers further changed. New particles with a smoother and rounder surface, with spherical geometry for PKT-VCM, were observed on the polymeric surface (PKT-VCM 0.64 ± 0.04 µm; PKSK-VCM 0.43 ± 0.04 µm). These particles are probably due to the presence of VCM in the samples.

3.4. Release of Vancomycin from PK Polymers

Different polymeric samples of PKSK and PKT loaded with VCM at different pH (PKT-VCM 2.3, 5.0, 8.8 and PKSK-VCM 2.3, 5.0, 8.8, see Figure 3) were employed for the study of VCM release at physiological pH 7.4, analogously to the procedure reported by Ruiz et al. for a formulation of VCM on surface-modified polypropylene[104]. According to data reported in Figure 3, it emerges that, PKSK-VCM release trends are rather similar, while a wider gap exists for release trends by PKT-VCM. Further, release of VCM from PKSK-VCM 5.0 is slower compared to PKSK-VCM 2.3 and 8.8, further suggesting the higher strength of the interactions formed between PKSK and VCM at this specific pH. On the contrary, release trends of VCM from PKT-VCM prepared at different pH, show

Preprints.org (www.preprints.org) | NOT PEER-REVIEWED | Posted: 19 June 2024 doi:10.20944/preprints202406.1370.v1

higher differences compared to those of PKSK-VCM, and the slowest release was obtained with PKT-VCM prepared at pH 2.3.

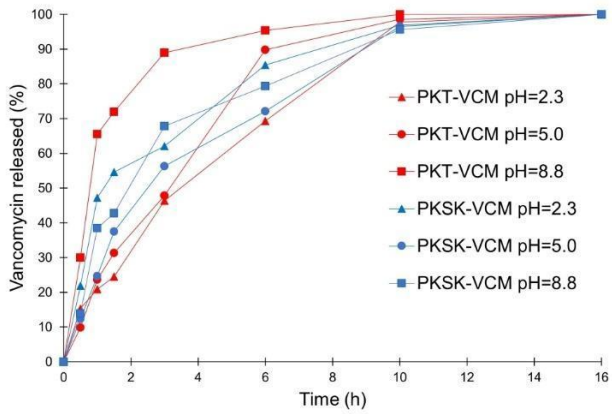

Figure 3. Vancomycin release at pH 7.4 from PKSK-VCM and PKT-VCM prepared at different pH (2.3, 5.0, 8.8).

The difference in VCM release profiles between PKSK and PKT could be ascribed to the different chemical composition of the post-functionalized polyketones. In fact, PKSK and PKT were deliberately modified with different functional groups (all bearing an SO_3-) but with different chemical backbones to highlight possible differences between aromatic (PKSK) and aliphatic (PKT) functionalities present. Some minor differences between the two polymers have been evidenced by FT-IR, but release tests clearly highlight the importance of the functional group present on the polymer. It may be speculated that not only ionic but also hydrophobic interactions between the aromatic functionality of sulfanilate and VCM, contribute to strengthen the interaction between the drug and the polymer.

3.5. Antimicrobial Tests

To test PKSK-VCM and PKT-VCM antibacterial activity, minimal inhibitory concentration (MIC) analyses were performed against Gram positive bacterial strains Staphylococcus aureus ATCC 25923 (MRSA), one of the main pathogens that can form biofilm infections [108,109]. Preliminarily PK, PKSK and PKT were tested against *Staphylococcus au*reus and their inefficacy verified (Figure 5S).

Data obtained from the antimicrobial tests carried out in the presence of PKSK-VCM and PKT-VCM are reported in Table 2 (corresponding growth curves Figure 6S). These data once more clearly show a significant dependence of the efficiency of VCM loading from the pH. In particular, loading at pH 5.0 allowed to achieve MIC values ~6 times lower than VCM alone, with both polymers, while PKSK-VCM and PKT-VCM loaded at pH 2.3 and 8.8 showed MIC values comparable to or higher than VCM alone.

Table 2. MIC values for PKSK-VCM and PKT-VCM loaded at variable pH, tested against Staphylococcus aureus ATCC 25923 (MRSA).

Sample	pH	MIC (μg/ml)
PKSK-VCM	2.3	1.44
PKSK-VCM	5.0	0.23
PKSK-VCM	8.8	1.56
PKT-VCM	2.3	2.68
PKT-VCM	5.0	0.24
PKT-VCM	8.8	3.79
VCM		1.54

Preprints.org (www.preprints.org) | NOT PEER-REVIEWED | Posted: 19 June 2024 doi:10.20944/preprints202406.1370.v1

4. Conclusions

In this work VCM has been successfully loaded on two polymers (PKT, PKSK) obtained from PK modified with the Paal-Knorr reaction using taurinate (T) and sulfanilate (SK). The loading of VCM was studied at three different pH, showing a substantial influence in the characteristics of the final polymeric formulation. Indeed, for both polymers the best EE% and LC% were obtained at pH 5.0 (for PKSK EE% 75.00, LC% 31.03; PKT EE% 80.00, LC% 31.58), together with prolonged release. Interestingly, MIC values obtained with PKSK-VCM and PKT-VCM were 6 times lower than those of VCM alone. These optimal achievements might be the result of different interactions between VCM and polymers that were supposed to involve both ionic and hydrophobic interactions. Moreover, pH used for loading has proved to be a very important variable, probably affecting the interactions occurring between the drug and the polymer. These results confirm the promising role of functionalized polyketones as DDS for VCM delivery and therefore further studies are ongoing to understand the influence of the polymer structure and the mechanisms of VCM loading, and the use of these polymers to produce transdermal patches for controlled release of Vancomycin. Moreover, the loading of different antibiotics on these polymers and their antibacterial activities will also be investigated.

Author Contributions: Conceptualization, Andrea Vavasori (A.V.), Rachele Rampazzo (R.R) and Valentina Beghetto (V.B.); methodology, A.V., Lucio Ronchin (L.R.), V.B., and R.R.; validation, Pietro Riello, Martina Marchiori (M.M.), Gloria Saorin (G.S.), V.B., and A.V.; formal analysis, A.V., RR and V.B.; investigation, M.M., R.R., G.S., V.B., and A.V.; resources, V.B., and A.V.; data curation, V.B., R.R., and A.V.; writing—original draft preparation, V.B. R.R.; writing—review and editing, V.B., and A.V, G.S.; visualization, A.V. and V.B.; supervision, V.B., and A.V.; project administration, V.B.; funding acquisition, V.B and A.V. All authors have read and agreed to the published version of the manuscript.

Funding: This research received no external funding.

Institutional Review Board Statement: Not applicable

Informed Consent Statement: Not applicable.

Data Availability Statement: the data presented in this study are available on request from the corresponding author.

Conflicts of Interest: The authors declare no conflicts of interest.

References

1. Morandini, A.; Spadati, E.; Leonetti, B.; Sole, R.; Gatto, V.; Rizzolio, F.; Beghetto, V. Sustainable triazine-derived quaternary ammonium salts as antimicrobial agents. RSC Adv. 2021, 11, 28092-28096. https://doi.org/10.1039/D1RA03455C.
2. Reece, R.; Beckwith, C. G. The Infectious Diseases Specialist, At Risk of Extinction. J. Infect. Dis. 2023, 228, 1649–1651. https://doi.org/10.1093/infdis/jiad160.
3. Momoh, A. O.; Asowata-Ayodele, A. M.; Olayemi, O.; David-Momoh, T. The comparative antimicrobial effects of castor, garlic, beniseed and bitter cola extracts on microorganisms isolated from hospitals' wards. Microbes Infect. 2023, in Press.
4. Shree, P.; Singh, C. K.; Sodhi, K. K.; Surya, J. N.; Singh, D. K. Bactericidal and biofilm eradication efficacy of a fluorinated benzimidazole derivative, TFBZ, against methicillin-resistant Staphylococcus aureus. Med. Microecol. 2023, 16, 100084. https://doi.org/10.3389/fphar.2024.1342821.
5. Liu, Z.; Deshazer, H.; Rice, A. J.; Chen, K.; Zhou, C.; Kallenbach, N. R.; Multivalent Antimicrobial Peptides as Therapeutics: Design Principles and Structural Diversities. J. Med. Chem. 2006, 49, 3436–3439. https://doi.org/10.1007/s10989-010-9230-z.
6. Bruni, G.; Maggi, L.; Tammaro, L.; Lorenzo, R. D.; Friuli, V.; D'Aniello, S.;. Maietta, M ; Berbenni, V.; Milanese, C.; Girella, A.; Marini, A.; Electrospun fibers as potential carrier systems for enhanced drug release of perphenazine. Int. J. Pharm. 2016, 511, 190–197. https://doi.org/10.1016/j.ijpharm.2016.07.011.
7. Gupta, A.; Makabenta, J. M. V.; Schlüter, F.; Landis, R. F.; Das, R.; Cuppels, M.; Rotello, V. M. Functionalized Polymers Enhance Permeability of Antibiotics in Gram-negative MDR Bacteria and Biofilms for Synergistic Antimicrobial Therapy. Adv. Ther. 2020, 3, 2000005. https://doi.org/10.1002/adtp.202000005.
8. Soto, S. M. Role of Efflux Pumps in the Antibiotic Resistance of Bacteria Embedded in a Biofilm. Virulence 2013, 4, 223–229. https://doi.org/10.4161/viru.23724.
9. Sharma, A., Gupta, V. K., Pathania, R. Efflux pump inhibitors for bacterial pathogens: From bench to bedside Indian J Med Res. 2019,149,129-145. https://doi.org/10.4103/ijmr.IJMR_2079_17.

Preprints.org (www.preprints.org) | NOT PEER-REVIEWED | Posted: 19 June 2024 doi:10.20944/preprints202406.1370.v1

10. Wang, T.; Rong, F.; Tang, Y.; Li, M.; Feng, T.; Zhou, Q.; Li, P.; Huang, W. Targeted polymer-based antibiotic delivery system: A promising option for treating bacterial infections via macromolecular approaches. Prog. Polym. Sci. 2021, 16, 101389. https://doi.org/10.1016/j.progpolymsci.2021.101389.
11. Liu, Y.; Li, R.; Xiao, X.; Wang, Z. Molecules that Inhibit Bacterial Resistance Enzymes. Molecules 2019, 24, 43. https://doi.org/10.3390/molecules24010043.
12. De Pascale, G.; Wright, G. D. Antibiotic resistance by enzyme inactivation: from mechanisms to solutions. Chembiochem 2010, 11, 1325–1334. https://doi.org/10.1002/cbic.201000067.
13. Zgurskaya, H. I.; Rybenkov, V. V. Permeability barriers of Gram-negative pathogens. Ann. N.Y. Acad. Sci. 2020, 1459, 5-18. https://doi.org/10.1111/nyas.14134.
14. Montanaro, L.; Campoccia, D.; Arciola, C. R. Advancements in molecular epidemiology of implant infections and future perspectives. Biomaterials 2007, 28, 5155-5168. https://doi.org/10.1016/j.biomaterials.2007.08.003.
15. Abebe, G. M. Detection of Biofilm Formation and Antibiotic Resistance in Klebsiella Oxytoca and Klebsiella Pneumoniae from Animal Origin Foods . Int. J. Microbiol. 2020, 2020. https://doi.org/10.11648/j.ijmb.20200503.17.
16. Das, A.; Patro, S.; Simnani, F. Z.; Singh, D.; Sinha, A.; Kumari, K.; Rao, P. V.; Singh, S.; Kaushik, N. K.; Panda, P. K.; Suar, M.; Verma, S. K. Biofilm modifiers: The disparity in paradigm of oral biofilm ecosystem. Biomed. Pharmacother. 2023, 164, 114966. https://doi.org/10.1016/j.biopha.2023.114966.
17. Venter, H.; Henningsen, M. L.; Begg, S. L. Antimicrobial resistance in healthcare, agriculture and the environment: the biochemistry behind the headlines. Essays Biochem. 2017, 61, 1–10. https://doi.org/10.1042/EBC20160053.
18. Rehman, S. A parallel and silent emerging pandemic: Antimicrobial resistance (AMR) amid COVID-19 pandemic. J. Infect. Public Health. 2023, 16, 611-617. https://doi.org/10.1016/j.jiph.2023.02.021.
19. Larsson, D. G. J.; Flach, C. F. Antibiotic resistance in the environment. Nat. Rev. Microbiol. 2022, 20, 257–269. https://doi.org/10.1038/s41579-021-00649-x.
20. Urban-Chmiel, R.; Marek, A.; Stępień-Pyśniak, D.; Wieczorek, K.; Dec, M.; Nowaczek, A.; Osek, Antibiotic Resistance in Bacteria-A Review. J. Antibiotics 2022, 11, 1079. https://doi.org/10.3390/antibiotics11081079.
21. Chin, K. W.; Michelle Tiong, H. L.; Luang-In, V.; Ma, N. L. The Role of Five-Membered Heterocycles in the Molecular Structure of Antibacterial Drugs Used in Therapy. Environ.Adv. 2023, 11, 100331. https://doi.org/10.3390/pharmaceutics15112554.
22. Morandini, A.; Leonetti, B.; Riello, P.; Sole, R.; Gatto, V.; Caligiuri, I.; Rizzolio, F.; Beghetto, V. Synthesis and Antimicrobial Evaluation of Bis-morpholine Triazine Quaternary Ammonium Salts. ChemMedChem 2021, 16, 3172–3176. https://doi.org/10.1002/cmdc.202100409.
23. Malaekeh-Nikouei, B.; Fazly Bazzaz, B. S.; Mirhadi, E.; Tajani, A. S.; Khameneh, B. The role of nanotechnology in combating biofilm-based antibiotic resistance. J Drug Deliv Sci Technol. 2020, 60, 101880. https://doi.org/10.1016/j.jddst.2020.101880.
24. Birk, S. E.; Boisen, A.; Nielsen, L. H. Polymeric nano- and microparticulate drug delivery systems for treatment of biofilms. Adv. Drug Deliv. Rev. 2021, 174, 30–52. https://doi.org/10.1016/j.addr.2021.04.005.
25. Sousa, A.; Phung, A. N.; Škalko-Basnet, N.; Obuobi, S. Smart delivery systems for microbial biofilm therapy: Dissecting design, drug release and toxicological features. J Control Release 2023, 354, 394–416. https://doi.org/10.1016/j.jconrel.2023.01.003.
26. Makhlouf, Z.; Ali, A. A.; Al-Sayah, M. H. Liposomes-Based Drug Delivery Systems of Anti-Biofilm Agents to Combat Bacterial Biofilm Formation. Antibiotics 2023, 12, 875. https://doi.org/10.3390/antibiotics12050875.
27. Sharma, S.; Mohler, J.; Mahajan, S. D.; Schwartz, S. A.; Bruggemann, L.; Aalinkeel, R. Microbial Biofilm: A Review on Formation, Infection, Antibiotic Resistance, Control Measures, and Innovative Treatment. Microorganisms 2023, 11, 1614. https://doi.org/10.3390/microorganisms11061614.
28. Elumalai, K.; Srinivasan, S.; Shanmugam, A. Review of the efficacy of nanoparticle-based drug delivery systems for cancer treatment. J. Biomed. Technol. 2024, 5, 109-122. https://doi.org/10.1016/j.bmt.2023.09.001.
29. Amidon, G. L.; Lennernäs, H.; Shah, V. P.; Crison, J. R. A theoretical basis for a biopharmaceutic drug classification: the correlation of in vitro drug product dissolution and in vivo bioavailability. Pharm. Res. 1995, 12, 413–420. https://doi.org/10.1023/a:1016212804288.
30. Patra, J. K.; Das, G.; Fraceto, L. F.; Campos, E. V. R.; Rodriguez-Torres, M. D. P.; Acosta-Torres, L. S.; Diaz-Torres, L. A.; Grillo, R.; Swamy, M. K.; Sharma, S.; Habtemariam, S.; Shin, H. S. Nano based drug delivery systems: recent developments and future prospects. J. Nanobiotechnology 2018, 16, 71. https://doi.org/10.1186/s12951-018-0392-8.
31. Al-Hussaniy, H. A.; Almajidi, Y. Q.; Oraibi, A. I.; Alkarawi, A. H. Nanoemulsions as medicinal components in insoluble medicines. Pharmacia 2023, 70, 537–547. https://doi.org/10.3897/pharmacia.70.e107131.
32. Yusuf, A.; Almotairy, A. R. Z.; Henidi, H.; Alshehri, O. Y.; Aldughaim, M. S. Nanoparticles as Drug Delivery Systems: A Review of the Implication of Nanoparticles' Physicochemical Properties on Responses in Biological Systems. Polymers 2023, 15, 1596. https://doi.org/10.3390/polym15071596.

Preprints.org (www.preprints.org) | NOT PEER-REVIEWED | Posted: 19 June 2024 doi:10.20944/preprints202406.1370.v1

33. Li, X.; Chen, Z.; Zhang, H.; Zhuang, Y.; Shen, H.; Chen, Y.; Zhao, Y.; Chen, B.; Xiao, Z.; Dai, J. Aligned Scaffolds with Biomolecular Gradients for Regenerative Medicine. Polymers 2019, 11, 341. https://doi.org/10.3390/polym11020341.
34. Adepu, S.; Ramakrishna, S. Controlled Drug Delivery Systems: Current Status and Future Directions Molecules 2021, 26, 5905. https://doi.org/10.3390/molecules26195905.
35. Ding, H.; Tan, P.; Fu, S.; Tian, X.; Zhang, H.; Ma, X.; Gu, Z.; Luo, K. Preparation and application of pH-responsive drug delivery systems. J. Control Release 2022, 348, 206–238. https://doi.org/10.1016/j.jconrel.2022.05.056.
36. Yadav, S. K.; Yadav, B.; Kumar Gupta, M.; Harish, S. A Comprehensive Review on Solid Dispersion Technique to Enhance the Solubility and Bioavailability of Poorly Water-Soluble Drugs. Int. J. Pharm. Res. 2023, 14, 106-117. https://www.ijppronline.com/index.php/IJPPR/article/view/313.
37. Sole, R.; Buranello, C.; Di Michele, A.; Beghetto, V. Boosting physical-mechanical properties of adipic acid/chitosan films by DMTMM cross-linking. Int. J. Biol. Macromol. 2022, 209, 2009–2019. https://doi.org/10.1016/j.ijbiomac.2022.04.181.
38. Singh, S.; Alrobaian, M. M.; Molugulu, N.; Agrawal, N.; Numan, A.; Kesharwani, P. Pyramid-Shaped PEG-PCL-PEG Polymeric-Based Model Systems for Site-Specific Drug Delivery of Vancomycin with Enhance Antibacterial Efficacy. ACS Omega 2020, 5, 11935–11945. https://doi.org/10.1021/acsomega.9b04064.
39. Park, M. R.; Seo, B. B.; Song, S. C. Dual ionic interaction system based on polyelectrolyte complex and ionic, injectable, and thermosensitive hydrogel for sustained release of human growth hormone. Biomaterials 2013, 34, 1327–1336. https://doi.org/10.1016/j.biomaterials.2012.10.033.
40. Palleria, C.; Di Paolo, A.; Giofrè, C.; Caglioti, C.; Leuzzi, G.; Siniscalchi, A.; De Sarro, G.; Gallelli, L. Pharmacokinetic drug-drug interaction and their implication in clinical management. J. Pharm. Sci. Res. 2013, 18, 601-10.
41. Stipa, P.; Marano, S.; Galeazzi, R.; Minnelli, C.; Mobbili, G.; Laudadio, E. Prediction of drug-carrier interactions of PLA and PLGA drug-loaded nanoparticles by molecular dynamics simulations. Eur. Polym. J. 2021, 147, 110292. https://doi.org/10.1016/j.eurpolymj.2021.110292.
42. Al Ragib, A.; Chakma, R.; Dewan, K.; Islam, T.; Kormoker, T.; Idris, A. M. Current advanced drug delivery systems: Challenges and potentialities. Int. J. Drug Deliv. Technol. 2022, 76, 103727. https://doi.org/10.1016/j.jddst.2022.103727.
43. Beghetto, V.; Gatto, V.; Conca, S.; Bardella, N.; Scrivanti, A. Polyamidoamide dendrimers and cross-linking agents for stabilized bioenzymatic resistant metal-free bovine collagen. Molecules 2019, 24, 3611–3622. https://doi.org/10.3390/molecules24193611.
44. Wang, M.- Q.; Zou, H.; Liu, W.-B.; Liu, N.; Wu, Z.-Q. Bottlebrush Polymers Based on RAFT and the "C1" Polymerization Method: Controlled Synthesis and Application in Anticancer Drug Delivery. ACS Macro Lett. 2022, 11, 179-185. https://doi.org/10.1021/acsmacrolett.1c00706.
45. Wang, C.; Zou, H.; Liu, N.; Wu, Z.- Q. Recent Advances in Polyallenes: Preparation, Self-Assembly, and Stimuli-Responsiveness. Chem. Asian J. 2021, 16, 3864. https://doi.org/10.1002/asia.202101051.
46. Zhao, S.- Q.; Hu, G.; Xu, X. – H.; Kang, S. – M.; Liu, N.; Wu, Z. – Q. Synthesis of Redox-Responsive Core Cross-Linked Micelles Carrying Optically Active Helical Poly(phenyl isocyanide) Arms and Their Applications in Drug Delivery. ACS Macro Lett. 2018, 7, 1073-1079. https://doi.org/10.1021/acsmacrolett.8b00610.
47. Larson, N.; Ghandehari, H. Polymeric Conjugates for Drug Delivery. Chem. Mater. 2012, 24, 840–853. https://doi.org/10.1021/cm2031569.
48. Irby, D.; Du, C.; Li, F. Lipid–Drug Conjugate for Enhancing Drug Delivery. Mol. Pharmaceutics. 2017, 14, 1325–1338. https://doi.org/10.1021/acs.molpharmaceut.6b01027.
49. Dalela, M.; Shrivastav, T. G.; Kharbanda, S.; Singh, H. pH-Sensitive Biocompatible Nanoparticles of Paclitaxel-Conjugated Poly(styrene-co-maleic acid) for Anticancer Drug Delivery in Solid Tumors of Syngeneic Mice. ACS Appl. Mater. Interfaces. 2015, 7, 26530–26548. https://doi.org/10.1021/acsami.5b07764.
50. Wu, F.; Jin, T. Polymer-Based Sustained-Release Dosage Forms for Protein Drugs, Challenges, and Recent Advances. AAPS PharmSciTech 2008, 9, 1218–1229. https://doi.org/10.1208/s12249-008-9148-3.
51. Mansour, A.; Romani, M.; Acharya, A. B.; Rahman, B.; Verron, E.; Badran, Z. Drug Delivery Systems in Regenerative Medicine: An Updated Review. Pharmaceutics 2023, 15, 695. https://doi.org/10.3390/pharmaceutics15020695.
52. Asadi, N.; Del Bakhshayesh, A. R.; Davaran, S.; Akbarzadeh, A. Common biocompatible polymeric materials for tissue engineering and regenerative medicine. Mater. Chem. Phys. 2020, 242, 122528. https://doi.org/10.1016/j.matchemphys.2019.122528.
53. Pei, X.; Wang, J.; Cong, Y.; Fu, J.; Recent progress in polymer hydrogel bioadhesives. J. Polym. Sci. 2021, 59, 1312–1337. https://doi.org/10.1002/pol.20210249.

Preprints.org (www.preprints.org) | NOT PEER-REVIEWED | Posted: 19 June 2024 doi:10.20944/preprints202406.1370.v1

54. Xu, R.; Fang, Y.; Zhang, Z.; Cao, Y.; Yan, Y.; Gan, L.; Xu, J.; Zhou, G. Recent Advances in Biodegradable and Biocompatible Synthetic Polymers Used in Skin Wound Healing. Mater. 2023, 16, 5459. https://doi.org/10.3390/ma16155459.
55. Zehetmaier, P. C.; Vagin, S. I.; Rieger, B. Functionalization of aliphatic polyketones. MRS Bull. 2013, 38, 239–244. https://doi.org/10.1557/mrs.2013.49.
56. Bartsch, G. C.; Malinova, V.; Volkmer, B. E.; Hautmann, R. E.; Rieger, B. Biokompatibilität von CO-Alkene-Polymeren mit aus urologischen Geweben isolierten primären Zellen und undifferenzierten Zellen. BJU Int. 2007, 99, 447–453. https://doi.org/10.1007/s00120-007-1493-4.
57. Knorr, L. Synthese von pyrrolderivaten. Ber. Dtsch. Chem. Ges. 1884, 17, 1635-1642. https://doi.org/10.1002/cber.18840170220.
58. Brubaker, M. M.; Coffman, D. D.; Hoehn, H. H. Synthesis and Characterization of Ethylene/Carbon Monoxide Copolymers, A New Class of Polyketones. J. Am. Chem. Soc. 1952, 74, 1509-1515. https://doi.org/10.1021/ja01126a047.
59. Chen, Q. – Y.; Wu, S. – W. Methyl Fluorosulphonyldifluoroacetate; a New Trifluoromethylating Agent. J. Chem. Soc. Chem. Commun., 1989, 11, 705-706. https://doi.org/10.1039/C39890000705.
60. Green, M. J.; Lucy, A. R.; Lu, S.; Paton, R. Functionalisation of alkene–carbon monoxide alternating copolymers via transketalisation reactions. J.Chem.Soc.Chem.Commun. 1994, 2063. DOI https://doi.org/10.1039/C39940002063.
61. Lu, S.; Paton, R. M.; Green, M. J.; Lucy, A. R. Synthesis and characterization of polyketoximes derived from alkene-carbon monoxide copolymers. Eur. Pol. J. 1996, 32, 1285. https://doi.org/10.1016/S0014-3057(97)80001-8.
62. Khansawai P., Paton, R. M.; Reed, D. Polyketones as alternating copolymers of carbon monoxide. Chem.Commun. 1999, 1297. https://doi.org/10.1070/rc2004v073n03abeh000840.
63. Nozaki, K.; Kosaka, N.;. Graubner, V. M; Hiyama, T. Methylenation of an Optically Active γ-Polyketone: Synthesis of a New Class of Hydrocarbon Polymers with Main-Chain Chirality. Macromol. 2001, 34, 6167–6168. https://doi.org/10.1021/ma0107713.
64. Reuter, P.; Fuhrmann, R.; Mucke, A.; Voegele, J.; Rieger, B.; Franke, R. P. Functionalization of aliphatic polyketones. Macromol. Biosci. 2003, 3, 123. https://doi.org/10.1557/mrs.2013.49.
65. Matteoli, U.; Beghetto, V.; Scrivanti, A.; Aversa, M.; Bertoldini, M.; Bovo, S. An alternative stereoselective synthesis of (R)- and (S)-Rosaphen® via asymmetric catalytic hydrogenation. Chirality 2011, 23, 779-783. https://doi.org/10.1002/chir.20989.
66. Araya-Hermosilla, R;. G. M. R.; Lima, Raffa, P.; Fortunato, G.; Pucci, A.; Flores, M. E.; Moreno-Villoslada I.; Broekhuis, A.A.; Picchioni, F. Intrinsic self-healing thermoset through covalent and hydrogen bonding interactions. Eur. Polym. J. 2016, 81, 186-197. https://doi.org/10.1016/j.eurpolymj.2016.06.004.
67. Ratna, D. Handbook of Thermoset Resins; Smithers Rapra: Shawbury, UK, 2009.
68. Vavasori, A.; Ronchin, L. Polyketones: Synthesis and Applications. In Encyclopedia of Polymer Science and Technology, 2017, pp 1–41.
69. Araya-Hermosilla, E.; Moreno-Villoslada, I.; Araya-Hermosilla, R.; Flores, M. E.; Raffa, P.; Biver, T.; Pucci, A.; Picchioni, F.; Mattoli, V. pH-Responsive Polyketone/5,10,15,20-Tetrakis-(Sulfonatophenyl)Porphyrin Supramolecular Submicron Colloidal Structures. Polymers 2020, 12, 2017. https://doi.org/10.3390/polym12092017.
70. Liu, N.; Zhou, L.; Wu, Z.- Q. Alkyne-Palladium(II)-Catalyzed Living Polymerization of Isocyanides: An Exploration of Diverse Structures and Functions. Acc.Chem.Res. 2021, 54, 3953–3967. https://doi.org/10.1021/acs.accounts.1c00489.
71. Liu, N.; Zhou, L.; Wu, Z. -Q. Helix-Induced Asymmetric Self-Assembly of π-Conjugated Block Copolymers: From Controlled Syntheses to Distinct Properties. Acc.Chem.Res. 2023, 56, 2954-2967. https://doi.org/10.1021/acs.accounts.3c00425.
72. Agostinelli, E.; Belli, F.; Tempera, G.; Mura, A.; Floris, G.; Toniolo, L.; Vavasori, A.; Fabris, S.; Momo, F.; Stevanato, R. Polyketone polymer: A new support for direct enzyme immobilization. J. Biotechnol. 2007, 127, 670–678. https://doi.org/10.1016/j.jbiotec.2006.08.011.
73. Araya-Hermosilla, E.; Parlanti, P.; Gemmi, M.; Mattoli, V.; Di Pietro, S.; Iacopini, D.; Granchi, C.; Turchi, B.; Fratini, F.; Di Bussolo, V.; Minutolo, F.; Picchioni, F.; Pucci, A. Functionalized aliphatic polyketones with germicide activity. RSC Advances. 2022, 12, 35358-35366. DOI https://doi.org/10.1039/D2RA06396D.
74. Cetinkaya, Y.; Falk, P.; Mayhall, C. G. Vancomycin-Resistant Enterococci Clin. Microbiol. Rev. 2000, 13, 686–707. https://doi.org/10.1128/cmr.13.4.686.
75. Levine, D. P. Vancomycin: A History. Clin. Infect. Dis. 2006, 42, S5–S12. https://doi.org/10.1086/491709.
76. Dinu, V.; Lu, Y.; Weston, N.; Lithgo, R.; Coupe, H.; Channell, G.; Adams, G. G.; Torcello Gómez, A.; Sabater, C.; Mackie, A.; Parmenter, C.; Fisk, I.; Phillips-Jones, M. K.; Harding, S. E. The antibiotic vancomycin induces complexation and aggregation of gastrointestinal and submaxillary mucins. Sci. Rep. 2020, 10, 960. https://doi.org/10.1038/s41598-020-57776-3.

Preprints.org (www.preprints.org) | NOT PEER-REVIEWED | Posted: 19 June 2024 doi:10.20944/preprints202406.1370.v1

77. Newman, D. J. Old and modern antibiotic structures with potential for today's infections. ADMET DMPK, 2022, 10, 131–146. https://doi.org/10.5599/admet.1272.
78. Ottonello, A.; Wyllie, J. A.; Yahiaoui, O.; Sun, S.; Koelln, R. A.; Homer, J. A.; Johnson, R. M.; Murray, E.; Williams, P.; Bolla, J. R.; Robinson, C. V.; Fallon, T.; Soares da Costa, T. P.; Moses, J. E. Shapeshifting bullvalene-linked vancomycin dimers as effective antibiotics against multidrug-resistant gram-positive bacteria. Proc. Natl. Acad. Sci. U.S.A. 2023, 120, e22087371. https://doi.org/10.1073/pnas.2208737120.
79. Willems, R. P. J.; Van Dijk, K.; Vehreschild, M. J. G. T.; Biehl, L. M.; Ket, J. C. F.; Remmelzwaal, S.; Vandenbroucke-Grauls, C. M. J. E. Incidence of infection with multidrug-resistant Gram-negative bacteria and vancomycin-resistant enterococci in carriers: a systematic review and meta-regression analysis. Lancet Infect. Dis. 2023, 23, 719–731. https://doi.org/10.1016/S1473-3099(22)00811-8.
80. O'Toole, R. F.; Leong, K. W. C.; Cumming, V.; Van Hal, S. Vancomycin-resistant Enterococcus faecium and the emergence of new sequence types associated with hospital infection. J. Res. Microbiol 2023, 174, 104046. https://doi.org/10.1016/j.resmic.2023.104046.
81. Li, X.; Hetjens, L.; Wolter, N.; Li, H.; Shi, X.; Pich, A. Charge-reversible and biodegradable chitosan-based microgels for lysozyme-triggered release of vancomycin. J. Adv. Res. 2023, 43, 87–96. https://doi.org/10.1016/j.jare.2022.02.014.
82. Iglesias-Mejuto, A.; Magariños, B.; Ferreira-Gonçalves, T.; Starbird-Pérez, R.; Álvarez-Lorenzo, C.; Reis, C. P.; Ardao, I.; García-González, C. A. Vancomycin-loaded methylcellulose aerogel scaffolds for advanced bone tissue engineering. Carbohydr. Polym. 2024, 324, 121536. https://doi.org/10.1016/j.carbpol.2023.121536.
83. Shi, Z.; Hu, Y.; Li, X. Polymer mechanochemistry in drug delivery: From controlled release to precise activation. J. Control Release 2024, 365, 259–273. https://doi.org/10.1016/j.jconrel.2023.10.042.
84. Zakeri-Milani, P.; Loveymi, B. D.; Jelvehgari, M.; Valizadeh, H. The characteristics and improved intestinal permeability of vancomycin PLGA-nanoparticles as colloidal drug delivery system. Colloids Surf. B. 2013, 103, 174–181. https://doi.org/10.1016/j.colsurfb.2012.10.021.
85. Yousry, C.; Elkheshen, S. A.; El-laithy, H. M.; Essam, T.; Fahmy, R. H. Studying the influence of formulation and process variables on Vancomycin-loaded polymeric nanoparticles as potential carrier for enhanced ophthalmic delivery. Eur. J. Pharm. Sci. 2017, 100, 142–154. https://doi.org/10.1016/j.ejps.2017.01.013.
86. Hassan, D.; Omolo, C. A.; Fasiku, V. O.; Mocktar, C.; Govender, T. Novel chitosan-based pH-responsive lipid-polymer hybrid nanovesicles (OLA-LPHVs) for delivery of vancomycin against methicillin-resistant Staphylococcus aureus infections. Int. J. Biol. Macromol. 2020, 147, 385–398. https://doi.org/10.1016/j.ijbiomac.2020.01.019.
87. Thamvasupong, P.; Viravaidya-Pasuwat, K. Controlled Release Mechanism of Vancomycin from Double-Layer Poly-L-Lactic Acid-Coated Implants for Prevention of Bacterial Infection. Polymers 2022, 14, 3493. https://doi.org/10.3390/polym14173493.
88. Sahiner, M.; Yilmaz, A. S.; Ayyala, R. S.; Sahiner, N. Carboxymethyl Chitosan Microgels for Sustained Delivery of Vancomycin and Long-Lasting Antibacterial Effects. Gels 2023, 9, 708. https://doi.org/10.3390/gels9090708.
89. Liu, W. -B.; Gao, R. -T.; Zhou, L.; Liu, N.; Chen, Z.; Wu, Z.-Q. Combination of vancomycin and guanidinium-functionalized helical polymers for synergistic antibacterial activity and biofilm ablation. Chem. Sci. 2022, 13, 10375-10382. https://doi.org/10.1039/D2SC03419K.
90. Sezer, A. D.; Kazak Sarılmışer, H.; Rayaman, E.; Çevikbaş A.; Öner, Akbuğa, E. T. J. Development and characterization of vancomycin-loaded levan-based microparticular system for drug delivery. Pharm Dev Technol. 2017, 22, 627-634. https://doi.org/10.3109/10837450.2015.1116564.
91. Vinod, L. A.; Rajendran, D.; Shivashankar, M.; Chandrasekaran, N. Surface interaction of vancomycin with polystyrene microplastics and its effect on human serum albumin. Int. J. Biol. Macromol. 2024, 256, 128491. https://doi.org/10.1016/j.ijbiomac.2023.128491.
92. Vavasori, A.; Ronchin, L.; Quartarone, G.; Tortato, C. The catalytic copolymerization of ethene with carbon monoxide efficiently carried out in water/dichloromethane/sodium dodecylsulfate emulsion. Modern Research in Catalysis 2013, 2, 93–99. https://dx.doi.org/10.4236/mrc.2013.23014.
93. Vavasori, A.; Ronchin, L.; Quartarone, G.; Tortato, C.; The catalytic copolymerization of ethene with carbon monoxide efficiently carried out in water/dichloromethane/sodium dodecylsulfate emulsion. Mod Res Catal. 2013, 2, 93-99. https://dx.doi.org/10.4236/mrc.2013.23014.
94. [94] Vavasori, A.; Toniolo, L. Carbon monoxide-ethylene copolymerization catalyzed by a Pd(AcO)2/dppp/TsOH1 system: the promoting effect of water and of the acid. J Mol Catal A Chem. 1996, 110, 13-23. https://doi.org/10.1016/1381-1169(96)00033-7.
95. [95] Ataollahi, N.; Girardi, F.; Cappelletto, E.; Vezzù, K.; Di Noto, V.; Scardi, P.; Callone, E.; Di Maggio, R. Chemical modification and structural rearrangements of polyketone-based polymer membrane. J. Appl. Polym. Sci. 2017, 134, 45485. https://doi.org/10.1002/app.45485.
96. [96] Ataollahi, N.; Vezzù, K.; Nawn, G.; Pace, G.; Cavinato, G.; Girardi, F.; Scardi, P.; Di Noto, V.; Di Maggio, R. A Polyketone-based Anion Exchange Membrane for Electrochemical Applications: Synthesis and Characterization. Electrochim. Acta. 2017, 226, 148–157. https://doi.org/10.1016/j.electacta.2016.12.150.

Preprints.org (www.preprints.org) | NOT PEER-REVIEWED | Posted: 19 June 2024 doi:10.20944/preprints202406.1370.v1

97. [97] Sole, R.; Gatto, V.; Conca, S.; Bardella, N.; Morandini, A.; Beghetto, V.;Sustainable Triazine-Based Dehydro-Condensation Agents for Amide Synthesis. Molecules, 2021, 26, 191-206. https://dx.doi.org/10.3390/molecules26010191.
98. Toncelli, C.; Schoonhoven, M. J.; Broekhuis, A. A.; Picchioni, F. Paal-Knorr kinetics in waterborne polyketone-based formulations as modulating cross-linking tool in electrodeposition coatings. Mater. Des. 2016, 108, 718–724. https://doi.org/10.1016/j.matdes.2016.06.127.
99. Scrivanti, A.; Sole, R.; Bortoluzzi, M.; Beghetto, V.; Bardella, N.; Dolmella, A. Synthesis of new triazolyl-oxazoline chiral ligands and study of their coordination to Pd(II) metal centers. Inorganica Chim. Acta 2019, 498, 119129. https://doi.org/10.1016/j.ica.2019.119129.
100. Ferreira, I. S.; Bettencourt, A. F.; Gonçalves, L. M. D.; Kasper, S.; Bétrisey, B.; Kikhney, J.; Moter, A.; Trampuz, A.; Almeida, A. J. Activity of daptomycin- and vancomycin-loaded poly-epsilon-caprolactone microparticles against mature staphylococcal biofilms. Nanomed. J. 2015, 10, 4351–4366. https://doi.org/10.2147/IJN.S84108.
101. [101] Le Ray, A.- M.; Chiffoleau, S.; Iooss, P.; Grimandi, G.; Gouyette, A.; Daculsi, G.; Merle, C. Vancomycin encapsulation in biodegradable poly(ε-caprolactone) microparticles for bone implantation. Influence of the formulation process on size, drug loading, in vitro release and cytocompatibility. Biomaterials. 2003, 24, 443-449. https://doi.org/10.1016/S0142-9612(02)00357-5.
102. [102] Honary, S.; Ebrahimi, P.; Hadianamrei, R. Optimization of particle size and encapsulation efficiency of vancomycin nanoparticles by response surface methodology. Pharm. Dev. Technol. 2014, 19, 987-998. https://doi.org/10.3109/10837450.2013.846375.
103. Kalhapure, R. S.; Mocktar, C.; Sikwal, D. R.; Sonawane, S. J.; Kathiravan, M. K.; Skelton, A.; Govender, T. Ion pairing with linoleic acid simultaneously enhances encapsulation efficiency and antibacterial activity of vancomycin in solid lipid nanoparticles. Colloids Surf B Biointerfaces. 2014,117, 303-311. https://doi.org/10.1016/j.colsurfb.2014.02.045.
104. Ruiz, J. C.; Alvarez-Lorenzo, C.; Taboada, P.; Burillo, G.; Bucio, E.; De Prijck, K.; Nelis, H. J.; Coenye, T.; Concheiro, A. Polypropylene grafted with smart polymers (PNIPAAm/PAAc) for loading and controlled release of vancomycin. Eur J Pharm Biopharm . 2008, 70, 467–477. https://doi.org/10.1016/j.ejpb.2008.05.020.
105. Takacs-Novak, K.; Noszal, B.; Tòkés-Kovesdi, M.; Sz6sz, G. Acid-base properties and proton-speciation of vancomycin. Int. J. Pharm. 1993, 89, 261-263. https://doi.org/10.1016/0378-5173(93)90252-B.
106. [106] Flores-Rojas, G. G.; Vázquez, E.; López-Saucedo, F.; Buendia-Gonzalez, L.; Vera-Graziano, R.; Mendizabal, E.; Bucio, E. Lignocellulosic membrane grafted with 4-vinylpiridine using radiation chemistry: antimicrobial activity of loaded vancomycin. Cellulose. 2023, 30, 3853–3868. https://doi.org/10.1007/s10570-023-05089-9.
107. Bil, M., Jurczyk-Kowalska, M.; Kopeć, K.; Heljak, M. Study of Correlation between Structure and Shape-Memory Effect/Drug-Release Profile of Polyurethane/Hydroxyapatite Composites for Antibacterial Implants. Polymers 2023, 15, 938. https://doi.org/10.3390/polym15040938.
108. Avila-Novoa, M. G.; Solis-Velazquez, O. A.; Guerrero-Medina, P. J.; González-Gómez, J. P.; González-Torres, B.; Velázquez-Suárez, N. Y.; Martínez-Chávez, L.; Martínez-Gonzáles, N. E.; De la Cruz-Color, L.; Ibarra-Velázquez, L. M.; Cardona-López, M. A.; Robles-García, M. A.; Gutiérrez-Lomelí, M. Genetic and compositional analysis of biofilm formed by Staphylococcus aureus isolated from food contact surfaces. Front. Microbiol. 2022, 13. https://doi.org/10.3389/fmicb.2022.1001700.
109. [109] Beghetto, V.; Gatto, V.; Samiolo, R.; Scolaro, C.; Brahimi, S.; Facchin, M.; Visco, A. Plastics today: Key challenges and EU strategies towards carbon neutrality: A review. Environmental Pollution, 2023, 334, 122102. https://doi.org/10.1016/j.envpol.2023.122102.

Disclaimer/Publisher's Note: The statements, opinions and data contained in all publications are solely those of the individual author(s) and contributor(s) and not of MDPI and/or the editor(s). MDPI and/or the editor(s) disclaim responsibility for any injury to people or property resulting from any ideas, methods, instructions or products referred to in the content.